

A comparison of exogenous labels for the histological identification of transplanted neural stem cells.

Francesca J. Nicholls^{1,2,4}, Jessie R. Liu³, & Michel Modo^{1,2,3}

¹University of Pittsburgh, McGowan Institute for Regenerative Medicine, Pittsburgh, USA

²University of Pittsburgh, Department of Radiology, Pittsburgh, PA15203, USA

³University of Pittsburgh, Department of Bioengineering, Pittsburgh, PA15203, USA

⁴Kings College London, Institute of Psychiatry, Department of Neuroscience, London, UK

Short title: Identifying transplanted cells.

Corresponding author:

Mike Modo

University of Pittsburgh

McGowan Institute for Regenerative Medicine &

Department of Radiology

3025 East Carson St

Pittsburgh, PA 15203

USA

+1 (412) 383 7200

modomm@upmc.edu

ABSTRACT

The interpretation of cell transplantation experiments is often dependent on the presence of an exogenous label for the identification of implanted cells. The exogenous labels Hoechst 33342, 5-Bromo-2'-deoxyuridine (BrdU), PKH26, and Qtracker were compared for their labeling efficiency, cellular effects and reliability to identify a human neural stem cell (hNSC) line implanted intracerebrally into the rat brain. Hoechst 33342 (2 mg/mL) exhibited a delayed cytotoxicity that killed all cells within 7 days. This label was hence not progressed to in vivo studies. PKH26 (5 μ M), Qtracker (15 nM) and BrdU (0.2 μ M) labeled 100% of the cell population at day 1, although BrdU labeling declined by day 7. BrdU and Qtracker exerted effects on proliferation and differentiation. PKH26 reduced viability and proliferation at day 1, but this normalized by day 7. In an in vitro co-culture assay all labels transferred to unlabeled cells. After transplantation, the reliability of exogenous labels was assessed against the gold standard of a human-specific nuclear antigen (HNA) antibody. BrdU, PKH26, and Qtracker resulted in a very small proportion (<2%) of false positives, but a significant amount of false negatives (~30%), with little change between 1 and 7 days. Exogenous labels can therefore be reliable to identify transplanted cells without exerting major cellular effects, but validation is required. The interpretation of cell transplantation experiments should be presented in the context of the label's limitations.

Keywords:

Neural stem cells, Cell transplantation, Hoechst, PKH26, Quantum Dots, Qtracker, BrdU, Validation, Proliferation, Differentiation, Toxicity, Phototoxicity, False Positive, False Negative, Reliability

Introduction

The correct identification of transplanted cells in host tissue is essential for the proper interpretation of cell therapy studies (13). Survival and differentiation of implanted cells can only be accurately assessed if grafted cells can be distinguished reliably from host cells (8). Hence, it is essential that the methods of identification are specific to implanted cells and are not transferred to host cells, potentially leading to a false positive identification and erroneous conclusion that implanted cells survived and differentiated into site-appropriate mature phenotypes (20,38). Conversely, if implanted cells cannot be readily detected inside the host tissue, an underestimation (i.e. false negatives) could lead to a misinterpretation of the effects of implanted cells on host tissue (77). The unambiguous interpretation of cell therapy is therefore highly dependent on a reliable identification of implanted cells (5,41).

The identification of implanted cells can be achieved by cell-specific characteristics that are different from the host tissue. Endogenous markers, such as the detection of the Y-chromosome of implanted male cells in female hosts (12,21) and antibodies against species-specific antigens (65,72) are the most reliable form of detection, but cannot always be applied, as in the case of syngeneic/alogeneic transplants, which constitute the most relevant clinical paradigms (12). Indeed, even the distinction of mouse cells in rat brains has proven difficult. The use of genetic reporters, such as LacZ (64,66) and green fluorescent proteins (26,29,42,58), can overcome some of these issues. Nevertheless, silencing of these genes upon differentiation (false negatives), as well as false positive detection limit their interpretation (61,69). A further concern for human studies is that genetic modification of cells can affect cellular characteristics (36), such as differentiation, or invoke an immunological response (1).

Exogenous markers that are non-permanently inserted into the cells for identification upon implantation provide an alternative in situations where endogenous markers cannot be used (13,54). For histological detection, a variety of exogenous labels are available ranging from histochemical dyes (e.g. Hoechst33342, FastBlue, carboxyfluorescein succinimidyl ester) (22,23,35,49,70) to fluorescent labels (e.g. PKH26, Dil, DiO, Quantum Dots) (19,22,40,73). A major concern with these exogenous labels is their potential to be exocytosed and lead to a false positive identification of host cells as transplanted cells (32). The validation of their reliability as markers of implanted cells remains a challenge and a “gold” standard is needed to distinguish host and implanted cells. A species-specific antibody against human cells in the rat brain can provide this

validation (4). Cellular effects of inorganic materials are also a concern (63,68). For instance, 5-Bromo-2'-deoxyuridine (BrdU) has been reported to affect neuronal differentiation (9,28), as well as being transferred to host cells (7,47,71). Only rarely do studies compare multiple labels in the same type of cell (22,31,60) and this has not, to our knowledge, been done for neural stem cells (NSCs).

To establish the reliability of different commonly used exogenous markers for the identification of NSCs after intracerebral implantation, the exogenous labels Hoechst, BrdU, PKH26, and Qtracker were compared for their cellular effects in vitro on a single human NSC line, in addition to validating the identification of implanted human cells in the rat brain against a gold standard detection using a species-specific antibody.

Materials and methods

Experimental Approach

To compare the reliability of different exogenous labels, a series of in vitro assays are conducted that provide Go/No-Go decision points to progress each label (Figure 1A). In vitro assays determined labeling efficiency, toxicity, as well as potential effects on proliferation and differentiation (Figure 1B), prior to evaluating their reliability after intracerebral implantation.

Human neural stem cell (NSC) line

The ganglionic eminence-derived NSC line STROC05 (ECACC accession number 04110301, ReNeuron) (24) (52) was cultured in tissue culture flasks coated with mouse laminin (10 µg/mL, Sigma-Aldrich, L2020) in serum-free medium supplemented with various factors (Table 1).

Cell Labeling

Labels were used according to the manufacturers' instructions, or as previously used for cell tracking. This resulted in a range of different conditions and incubation times (Figure 1C). Exogenous labels target different sub-cellular structures and hence might exert different cellular effects and have different propensities for exocytosis (Figure 1D).

| Component | Source | Final Concentration |
|-----------------------------|---------------------|---------------------|
| Human Albumin Solution | GemBio 800-121 | 0.03 % |
| Transferrin, human | Sigma T1147 | 100 µg/mL |
| Putrescine DiHCl | Sigma P5780 | 16.2 µg/mL |
| Insulin, human recomb. | Sigma I9278 | 5 µg/mL |
| L-Thyroxine (T4) | Sigma T0397 | 400 ng/mL |
| Tri-iodo-thyronine (T3) | Sigma T6397 | 337 ng/mL |
| Progesterone | Sigma P8783 | 60 ng/mL |
| L-glutamine | Sigma G7513 | 2 mM |
| Sodium Selenite | Sigma S9133 | 40 ng/mL |
| Heparin Sodium | Sigma H3149 | 10 units/mL |
| Corticosterone | Sigma C2505 | 40 ng/mL |
| bFGF | PeptoTech 100-18B | 10 ng/mL |
| EGF | PeptoTech AF-100-15 | 20 ng/mL |
| 4-hydroxy-tamoxifen (4-OHT) | Sigma H7904 | 100 nM |

Table 1. Components added to DMEM-F12 basal medium for STROC05 proliferation medium. For differentiation medium, bFGF, EGF and 4-hydroxy-tamoxifen were omitted.

Hoechst 33342. Hoechst binds to the AT rich minor groove of DNA, with an excitation peak at 346 nm and emission at 460 nm (74). A stock solution of Hoechst 33342 (2 mg/mL, Sigma) (23,48,57) was added to cells at 1:1000 for a final concentration of 2 µg/mL for 30 minutes. Cells were washed 3x with Hank's Balanced Salt Solution (HBSS) before being harvested. Due to the toxicity of Hoechst to this cell line, dilutions down to 0.02 µg/mL were tested, but a similar cell loss was observed. However, endothelial cells were unaffected (Data not shown).

5-Bromo-2'-Deoxyuridine (BrdU). BrdU is incorporated into DNA, replacing Thymidine, during DNA replication, which occurs during cell proliferation and repair (71). It is detected using antibodies, so the excitation/emission can be tailored as required. For this study, we used Alexa Fluor 555, with excitation at 555 nm and emission at 580 nm. A stock solution of BrdU (50 mM) was diluted 1:250 (0.2 mM) and filtered (0.22 µm pore size) prior to addition to growing cells at 0.2 µM at 37 °C (9). BrdU-supplemented media was replaced twice a day for four days.

PKH26. PKH26 is a lipophilic dye that is incorporated into lipid regions of the cell membrane. As it becomes internalized during endocytosis, it is also incorporated into

organelle membranes, giving its punctate appearance (46). PKH26 excitation peaks at 551 nm with emission at 567 nm. As previously reported (39,40), cells were suspended (5×10^5 cells/mL) in PKH26 solution at a final concentration of 5 μ M PKH26 in Diluent C for 4 minutes. An equivalent volume of human albumin solution (1%, Biosera) was added, and incubated for a further 1 minute prior to 3x washes in DMEM/F12.

Quantum Dots. The Qtracker system consists of Qdot nanocrystals (10-20 nm) coated with a proprietary targeting peptide for localization to the cytoplasm (34). Qtracker 565 (Life Technologies) excitation peaks at 405-525 nm and emission at 565 nm. Qtracker 565 was prepared by mixing components A and B for 5 min at room temperature. Qtracker (15 nM) and human albumin serum (2%) in media was vortexed for 1 min prior to incubation with cells for 24 h at 37 °C. Cells were washed 2x and incubated in fresh media at 37 °C for 2.5 h.

In vitro studies of cellular effects

Acute Toxicity. Trypan blue dye is excluded from viable cells with an intact membrane, whereas dead or dying cells are permeable to the dye. Equal amounts of cell suspension and Trypan blue solution were thoroughly mixed. Counts of total cells and dead cells were taken on a hemacytometer and expressed as a percentage of viable cells.

Phototoxicity. Certain exogenous labels can induce toxicity through their interaction with light (59). This phototoxicity has previously been reported for PKH26 (45), Hoechst (33) and others (55,60). For this, cells were labeled and seeded at 1×10^5 cells/well prior to exposure to either ambient light in the tissue culture hood for one hour, or fluorescent light for 5 min at the label's excitation wavelength, or using DAPI filters for unlabeled and BrdU cells. Control conditions were included where cells either remained in the incubator, or were left in the hood without light exposure, to control for effects of temperature and CO₂ variation.

All wells were returned to the incubator overnight. Using a Lactate Dehydrogenase (LDH) cytotoxicity assay kit (Pierce, Thermo Scientific), cells were assessed for membrane damage leading to cell death. Supernatant (50 μ L) was removed from each well to provide a measure of LDH released due to cell death or membrane damage. To provide a measure of maximal LDH release and control for cell number variation, lysis buffer was added for 45 min to the remaining media to lyse all cells. To measure background activity in the media, fresh media was also included. The LDH dye was added and allowed to react for 30 min at room temperature in the dark before stop solution was

added. Absorbance was measured at 490 nm with background (680 nm) subtracted. Cytotoxicity was calculated as:

$$\% \text{ Cytotoxicity} = \frac{\text{LDH release} - \text{media background}}{\text{Max LDH} + \text{LDH release} - \text{media background}} \times 100$$

Cell viability/Acute toxicity - Live/Dead. Live cells were detected with green fluorescent calcein-AM (intracellular esterase activity, Invitrogen), whereas the red ethidium homodimer-1 (EthD-1) indicated dead or dying cells. For this, cells (1×10^5 cells/well) in proliferation medium were cultured for 24 hours at 37 °C prior to addition of 4 μM EthD-1 and 2 μM Calcein AM (in PBS, 300 μL) for 30 min in the dark. Cells were then live imaged immediately.

Cell survival/chronic toxicity. After labeling, cells were cultured for 24 h in proliferation medium. Cells for the Day 1 time point were then fixed, while cells for the day 7 time point were transferred into differentiation medium and cultured for a further 7 days. The total number of DAPI stained nuclei was counted over 9 fields of view per coverslip (445 x 335 μm , 20X objective) and compared to unlabeled STROC05.

Cell Proliferation. The number of Ki67 positive cells was expressed as a percentage of DAPI nuclei, giving the percentage of cells expressing this marker of proliferation.

Cell Differentiation. To assess effects on differentiation, cells were stained with GFAP (Glial Fibrillary Acidic Protein, a marker of astrocytic lineage), Tuj1 (Neuronal class III beta-tubulin, a marker of early neuronal lineage) and Galc (Galactocerebroside, an oligodendrocyte marker) (see Immunocytochemistry below). The number of cells staining positively for each of these markers was expressed as a percentage of DAPI+ cells, counted over 5 fields of view per coverslip.

In vitro label transfer

In order to assess label leakage in vitro, NSCs were labeled, cultured overnight, and then mixed with unlabeled endothelial cells (1:1 ratio) in suspension before seeding the mixture into wells. The immortalized human cerebral microvascular endothelial cell line (hCMEC/D3) (10,75) was cultured in tissue culture flasks (BD Biosciences) coated with rat tail collagen type I (150 $\mu\text{g/mL}$, BD Biosciences, 354236) using endothelial basal medium-2 (EBM-2; Lonza), supplemented with various factors (Table 2). The media and coating for the two cell types were mixed in a 1:1 ratio (11). After 24 hours, cultures were

stained for nestin, which is present in NSCs, but not ECs. Therefore co-localization of nestin and the tested label indicates correct identification, whereas the presence of the label in a nestin negative cell indicates label leakage. In order to rule out the possibility that observed results were only due to mechanical transfer between cells during the pipetting process, other paradigms were investigated.

| Component | Final Concentration | Supplier |
|--------------------------------------|---------------------|-------------------|
| EBM-2 | Basal medium | Lonza |
| Fetal Bovine Serum "Gold" | 5% | PAA |
| Chemically defined lipid concentrate | 1% | Life Technologies |
| Penicillin-Streptomycin | 1% | Sigma-Aldrich |
| HEPES | 10 mM | Sigma-Aldrich |
| Ascorbic Acid | 5 µg/ml | Sigma-Aldrich |
| bFGF | 1 ng/ml | PeptoTech |
| Hydrocortisone | 1.4 µM | Sigma-Aldrich |

Table 2. hCMEC/D3 medium components.

Immunocytochemistry

Cells were rinsed twice with HBSS before being incubated for 15 min with cold 4% paraformaldehyde (PFA). Coverslips were washed 3x5 min in PBS and incubated in blocking solution (PBS + 10% Normal Goat Serum, Vector Labs + 0.1% Triton-X100, Sigma) for 1 hour (hr) at room temperature. Primary antibodies were applied overnight (Table 3) prior to incubation with appropriate AlexaFluor secondary antibodies (1:500, Molecular Probes) for 1 hr at room temperature and washed 3x5 min in PBS. Coverslips were mounted onto slides with Vectashield+DAPI mounting medium (Vector Labs). Visualization of BrdU required a 2-step procedure. Immunocytochemistry for other antibodies was performed first, followed by an additional fixation with 4% PFA for 20 min to preserve the previous staining. After 3x5 min washes with PBS, an acid treatment to denature the DNA afforded binding of the BrdU antibody. Coverslips were incubated on ice for 10 min with 1.0 M HCl (Hydrochloric Acid, Sigma), then 10 min at room temperature in 2.0 M HCl followed by 20 min in 2.0 M HCl at 37 °C. To neutralize the acid, 0.1 M Borate buffer (Sodium tetraborate decahydrate, Sigma) was applied for 12 min at room

temperature. Overnight incubation with the BrdU antibody (rat anti-BrdU, 1:5,000, AbD Serotec) and the relevant AlexaFluor secondary were completed as described above.

| Antibody | Concentration | Company | Cat. Ref. |
|-----------------|----------------------|--------------------|------------------|
| BrdU | 1:5000 | AbD Serotec | MCA2060T |
| Galc | 1:300 | Millipore | MAB342 |
| GFAP | 1:3000 | Sigma | G3893 |
| HNA | 1:400 | Chemicon | MAB1281 |
| HSP27 | 1:200 | Enzo Life Sciences | SPA-803 |
| Ki67 | 1:500 | Abcam | ab15580 |
| Nestin | 1:2000 | Millipore | MAB5326 |
| Sox2 | 1:500 | Santa Cruz | sc-17320 |
| STEM101 | 1:500 | Stem Cells Inc. | AB-101-U-050 |
| Tuj | 1:500 | Abcam | ab18207 |

Table 3. Antibodies and concentrations used for immunocytochemistry and immunohistochemistry.

In vivo cell transplantation

Animals. Male Sprague-Dawley rats (180-200 g, Taconic) were allowed 7 days of acclimatization prior to cell transplantation. Each animal received one cell transplantation into each hemisphere, each consisting of a different label (n=5 per label/time point). Animals were perfused at 1 and 7 days post-transplantation. All procedures complied with the Institutional Animal Care and Use Committee, as well as NIH guidelines.

Cell Preparation. All labeling was performed using the same concentration and procedures than for in vitro studies. To reduce potential in vivo leakage (27), labeled and washed cells were incubated overnight in fresh proliferation medium. Cells were washed 3x with HBSS before being harvested and re-suspended in PBS to achieve a cell density of 50,000 cells/ μ L using the following formula (56):

$$V_L = V_T - V_C$$

Where V_L = volume of liquid to be added; V_T = total desired volume of suspension (μ L);

V_C = Cell Volume = Total cell number x 3.912 pL (volume of 1 cell)

Adjustments were made if the density was more than 10% different from the target density. A consistent high viability of >85% for 7 hours was maintained when cells were kept at room temperature after suspension at 50,000 cells/ μ L. Samples of injected cell suspensions were measured for cell viability (trypan blue) before and after each surgery,

as transplantation of dead cells is known to have effects on label leakage and re-uptake (7). For each animal, separate aliquots were prepared to minimize potential density variations and loss of viability due to repeated re-suspension.

Stereotactic Surgery. Using isoflurane anesthesia (4% induction, 2% maintenance in medical air), animals were secured in a stereotactic frame (Kopf). Under aseptic conditions, a frame-mounted drill (Foredom) was used to make small burr holes in the skull at -0.9 mm anterior and ± 2.5 mm laterally to Bregma with deposits delivered -6 mm ventrally to the surface of the cortex. The cell suspension was briefly pipetted (5x) to re-suspend cells (5 μ L) in a 10 μ L Hamilton syringe. For each exogenous label, separate syringes were used to avoid cross contamination. The syringe was attached to the frame and the 26 G needle was inserted slowly to 5.5 mm below the dura. 4 μ L of cell suspension (total ~200,000 cells) was then injected at 1 μ L/min using a frame-mounted automated microinjector (Micro4, WPI). The needle was left in place for an additional two minutes before being slowly removed. Each animal received two injections of a single deposit (different experimental groups), one in each hemisphere. The two burr holes were then sealed with bone wax (Fisher) before the incision was sutured. Animals were given topical analgesic cream (2.5% Lidocaine and 2.5% Prilocaine, Sandoz) and Buprenex (0.05 mg/kg i.p.; Henry Schein).

Perfusion-fixation. Animals were given i.p. injections of Pentobarbital Sodium (10 mg/100 g b.w., Fatal Plus, Vortech) until all reflexes were absent. Ice cold PBS (0.01 M) was perfused transcardially to flush blood out of the system, followed by ice cold paraformaldehyde (4% in 0.01 M PBS). Brains were excised and post-fixed in 4% PFA overnight before being cryoprotected in 30% sucrose with 0.5% Sodium Azide.

Immunohistochemistry

Brains were cut at 40 μ m section thickness on a cryostat (Leica) and stored in Tissue Cryopreservation Solution (TCS, 30% Ethylene Glycol, 25% Glycerol and 0.5% Sodium Azide in PBS) to prevent freezing at -20 °C. Immunohistochemistry followed the same procedure as immunocytochemistry, except that after secondary antibodies were removed, sections were counterstained with the nuclear marker Hoechst (1 μ g/mL in PBS, Sigma) for 5 min and Vectashield mounting medium was used.

Image analysis

Using an AxioImager M2 microscope (Zeiss, 20X objective) with Stereo Investigator software (MBF), the first, last and center sections containing HNA+ cells were chosen as a representative coverage of the graft with Hoechst+, HNA+ and/or exogenous labels counted using ImageJ64. Cells (Hoechst+) were categorized as “correctly identified” if both HNA and the label were present, “false negative” cells were defined as HNA+ without an exogenous label, whereas “false positive” cells contained an exogenous labeled but were HNA- (44) (Figure 1E).

Statistics

Statistical tests were performed using Prism 5.0f (GraphPad). A non-parametric Mann-Whitney test was used to compare each group of labeled cells with its matching control, whereas a Friedman test with Dunn’s multiple comparison test was used to analyze cell viability over time. For in vivo analyses, Kruskal-Wallis tests were used with Dunn’s multiple comparison test. For in vitro assays, three biological replicates, each with three technical replicates were conducted to give n=9. For in vivo analysis, n=5 per label per time point.

Results

Efficiency of cell labeling and toxicity

Exogenous labels are inherently different in their biophysical properties, influencing the uptake characteristics of the agents into the cells, as well as their intra-cellular localization. Specifically, Hoechst and BrdU are both bound to DNA and are therefore localized to the nucleus of a cell (Figure 2A). In contrast, PKH26 and Qtracker are cytoplasmic with some evidence of membrane labeling. Hoechst and BrdU show continuous labeling throughout the nucleus, whereas PKH26 and Qtracker show punctate fluorescence throughout the cell body. All exogenous labels allow a robust in vitro labeling that affords the visualization of a population of cells (Figure 2B). Label efficiency is high with ~100% of cells labeled for all labels at day 1. At day 7, PKH26 and Qtracker maintain their high efficiency, whereas BrdU declines significantly ($p<.01$) to 87% (Figure 2C). A major challenge to the BrdU labeling is that it is only taken-up into dividing cells. Since the other labels permeate into both dividing and non-dividing cells, they appear more consistent across the population and are not as readily diluted. BrdU hence constitutes the least efficient exogenous label.

BrdU contrasts with Hoechst, PKH26 and Qtracker in that it requires an antibody for detection. All other labels have inherent fluorescent properties that afford easy

identification, but also potentially renders them phototoxic. However, no phototoxicity was evident with BrdU, PKH26 or Qtracker in comparison to control conditions (LDH assay, Figure 2D). There was also no significant acute toxicity as indicated by viability of cells after labeling without light exposure being comparable to controls (Figure 3A). Only an acute 4% decrease in live cells ($p < .05$) was evident after PKH26 labeling (Figure 3B). At 24 hrs, an equivalent level of live cells was present in all conditions. These results indicate that none of the labels induces an acute toxicity. However, dead cells are removed from the culture during media changes, and these assays may not be sufficient to demonstrate an absence of toxicity.

Effects on cellular functions

The most dramatic cellular effects were seen on cell proliferation and survival (Figure 4A). Indeed, Hoechst labeling dramatically affected both proliferation ($p < .001$) and survival ($p < .01$) at day 1 (Figure 4B). By day 7, only very few cells survived ($p < .001$) compared to unlabeled controls. In contrast, BrdU exerted no significant effect on survival at day 1 or 7 (Figure 4C), although a small increase in proliferation was evident at day 1 ($p < .05$) which normalized again by day 7. On day 1, PKH26 decreased proliferation ($p < .001$), but overall more cells were evident ($p < .05$, Figure 4D). This opposing effect normalized by day 7. For Qtracker, both proliferation and total number of cells ($p < .001$) were elevated at day 1 (Figure 4E). By 7 days, cell number remained elevated ($p < .001$), but proliferation was reduced ($p < .001$). These results indicate that Hoechst exerts a delayed toxic effect on cells and hence this label was not included in further assessments.

A further key function of NSCs is their ability to differentiate into neurons, astrocytes and oligodendrocytes (Figure 5A). BrdU decreased the presence of GFAP+ cells at day 1 and day 7 ($p < .05$), but not Tuj (Figure 5B). GalC was transiently increased at day 1 ($p < .01$), but the difference from controls was smaller ($p < .05$) by day 7. In contrast, PKH26 labeled cells were equivalent to controls at day 1. By day 7, there was a slight increase in GFAP+ cells ($p < .01$) and a decrease in Tuj and GalC cells ($p < .05$) (Figure 5C). Qtracker exerted the most significant increase in GFAP expression ($p < .001$, Figure 5D), with no effects on Tuj, and a slight decrease in GalC+ cells at 7 days ($p < .05$). These results indicate that all 3 exogenous labels exerted some effects on NSC differentiation, with PKH26 exerting the least effects, compared to Qtracker having the strongest effect on GFAP+ cells (20-40% increase). However, both PKH26 and Qtracker appear to significantly alter the morphology of astrocytes (Figure 5A).

In vitro label transfer to unlabeled cells

To determine the potential transfer of label from labeled NSCs to unlabeled endothelial cells (ECs), a variety of assays were employed, such as co-plating, plating of unlabeled cells first, plating of labeled cells first, as well as use of conditioned media from labeled cells (Figure 6A). Hence transfer of the label from Nestin-positive NSCs to ECs was indicated by the presence of exogenous label in ECs. In all cases, transfer of PKH26 occurred with 100% of unlabeled ECs containing PKH26. To compare the potential transfer of different labels, labeled NSCs were co-plated with unlabeled endothelial cells (ECs). After 24 hours of co-culture, transfer of label was evident for Hoechst, PKH26, and Qtracker with all ECs containing label (Figure 6B). However, only ~70% of unlabeled ECs were labeled with BrdU. These results therefore indicate that a significant label transfer occurs in vitro between labeled and unlabeled cells. This suggests that these labels have a high potential to generate false positive identification after transplantation.

In vivo identification of implanted cells

To ensure equivalent delivery of the number of cells, a quality control of the cell suspensions was performed to ensure that these were within a 10% error margin of the target concentration (Figure 7A) and that their viability was maintained at room temperature (Figure 7B). This resulted with all labels having a viability of ~90% at the start of the transplantation procedure and >85% at the end of the procedure (Figure 7). Hence a consistent number of labeled cells was administered with a minimal number of dead cells being contained within the injectate.

To validate the reliability of exogenous labels for the detection of transplanted NSCs in the brain, it is essential to establish a “gold” standard such as detecting human antigens. In vitro, human nuclei antigen (HNA), human specific heat shock protein 27 (HSP27) and SC101, all reliably visualize 100% of human NSCs (Figure 7D) and cells in adult human hippocampal tissue indicating their sensitivity to detect human cells (Figure 7E). In contrast, in normal rat brain, the antibody does not result in any staining of cells (Figure 7F), indicating the antibody’s specificity for human cells. The correct identification of transplanted cells using exogenous labels was validated against HNA staining to define correctly identified cells, false negatives, as well as false positives (Figure 7G).

The identification of human NSCs in the brain based on exogenous markers can therefore be compared to their detection by HNA at 1 and 7 days post-transplantation

(Figure 8). The overall location and detection of “grafts” based on BrdU, PKH26, and Qtracker was accurate with no evidence of a significant amount of exogenous label outside of the transplant area. Although macroscopically exogenous labels might hence accurately report on the location and distribution of the transplanted cells, uptake of exogenous label in host cells could lead to a mistaken identification of individual implanted cells, potentially leading to an erroneous interpretation of cellular phenotypes. Consequently, for each label, it is essential to establish what proportion of implanted cells (based on HNA staining) is correctly identified, but also establish to what degree false negatives and positives could affect the interpretation of cell transplantation experiments (Figure 9A). Approximately 60% of implanted cells were correctly identified using exogenous labels on day 1 and 7 (Figure 9B). On day 7, PKH26 was significantly less reliable in identifying implanted cells compared to Qtracker ($p < .05$), but there was no significant decrease in the reliability of cell identification for PKH26 between day 1 and 7. Conversely, ~35% of implanted cells resulted in false negatives for all labels (Figure 9C). Again PKH26, at 7 days post-implantation, resulted in a significantly higher amount of false negatives compared to Qtracker ($p < .05$). Surprisingly, in vivo very few (<2%) false positives were evident for all labels (Figure 9D), contradicting results of the in vitro experiments. Individual transplanted cells can hence be reliably identified histologically based on exogenous labels, but there is a significant problem of underestimating the total number of implanted cells.

Discussion

The interpretation of intracerebral cell transplantation experiments is dependent on the reliable identification of implanted cells. The use of exogenous labels potentially leads to an under- or overestimation of implanted cells and labeling itself might exert ill-effects on cellular functions. We here evaluated and compared different exogenous labels for their uptake efficiency, cellular effects, as well as reliability for in situ histological identification (Table 4).

| | | Hoechst | BrdU | PKH26 | Qtracker |
|---------------------------|------------------------|---------|------|-------|----------|
| Ease of labeling protocol | | ++ | + | ++ | ++ |
| In vitro | Labeling Efficiency | ++ | + | ++ | ++ |
| | Toxicity (acute) | + | ++ | + | ++ |
| | Cell Survival | - - | ++ | ++ | + |
| | Phenotype | n/a | + | + | + |
| | Label Transfer | - - | - | - - | - - |
| In vivo | False +ve | n/a | ++ | + | + |
| | False -ve | n/a | - | - | - |
| | Ease of identification | n/a | ++ | + | + |

Table 4. Summary of strengths and weaknesses for consideration of using tested exogenous labels (++ = Excellent, + = Good, - = Fair, - - = Poor)

The reliability of exogenous labels for cell identification

The identification of transplanted cells is dependent on efficient labeling of cells in vitro. Hoechst, PKH26 and Qtracker efficiently labeled 100% cells and were easy to detect inside the cells in vitro. Only PKH26 and Qtracker progressed to in vivo studies and although their fluorescence was easily detected for macroscopic localization of grafted cells, establishing co-labeling of specific cells is more challenging due to the distributed punctate nature of the exogenous labels. Indeed, non-cytoplasmic antibodies, such as GFAP, complicate a clear co-localization of these cell identification markers with phenotypic markers. BrdU labeling dropped to 87% of cells after 7 days despite 4 days of incubation, the longest duration of all exogenous labels. Indeed, the duration and immunohistochemical procedure to visualize BrdU complicate its use for cell transplantation studies. However, its nuclear localization made it much easier to definitively identify in vivo, where it was sometimes unclear with cytoplasmic labels to which nucleus they belonged.

PKH26 and Qtracker's punctate appearance is strong, but can also be confused with dust particles or other histological artifacts, such as lipofuscin (37), if not associated with a cell or a sufficient amount of particles being visible. Individual punctate fluorescence dots in the interstitial space are hence ignored, but could indicate exocytosis of the agent from labeled cells. There is a clear indication of label transfer being a potential issue, as the co-culture here with unlabeled cells indicated a major transfer from labeled cells for both PKH26 and Qtracker. PKH26, being incorporated into the membrane, would

necessarily be exocytosed during normal membrane turnover, so this effect cannot easily be attenuated. For Qtracker, the targeting mechanism is proprietary, so the method of label transfer cannot easily be inferred. BrdU, which is meant to stably insert into the DNA of labeled cells, showed a lower level of transfer, as observed by others (7,47). The fusion of some labeled cells with unlabeled cells could account for a proportion of double-labeling and hybrid cells (6), but is unlikely to account for an almost 100% transfer rate. Although this assay clearly demonstrated the potential for label transfer (3,16), the predictability of this co-culture for in vivo studies is questionable, as there were very few (<2%) false positives found in vivo for BrdU, PKH26 or Qtracker. Other studies reported 5-20% false positives (4,7,32,47), but a key difference is that labeled cells here were incubated overnight prior to transplantation. This has been demonstrated previously to significantly reduce the leakage of an exogenous label (27). Albeit the fusion of labeled cells with host cells can lead to a misinterpretation of transplanted NSCs (6), results here indicate that this is unlikely. A more significant issue is potentially autofluorescent signals in brain tissue, including lipofuscin, which can complicate the unambiguous detection of transplanted cells in the absence of a gold standard (37,69). Our results here suggest that the use of exogenous labels is potentially reliable to study the phenotypic differentiation of transplanted cells, but labels, such as PKH26 and Qtracker, are difficult to co-localize to yield an unequivocal interpretation of cell phenotypes.

A major issue that was apparent here is the high proportion of false negatives for all labels investigated. Approximately 30% of cells that were transplanted even at day 1 were not detectable based on the exogenous label. Considering that label efficiency was 100% at day 1, a smaller degree of false negatives could be expected. False negatives can potentially be due to dilution of label through cell division, but this is unlikely 24 h post-transplantation and hence cannot account for the high proportion of unlabeled cells here. Although photobleaching (i.e. reduction in fluorescent activity due to prolonged light exposure) could account for a decrease in fluorescent label detection (30,50), Qtracker is not thought to be susceptible to photobleaching (18,78). Processing of tissue for immunohistochemistry can potentially also affect exogenous labels. A further alternative explanation is that cell counts here in tissue sections based on HNA overestimate the number of transplanted cells. However, we previously demonstrated that HNA-based stereological cell counts are equivalent with an estimation of cell counts based on Alu-qPCR (66) and there is no cross-reactivity with rat cells. The high rate of false negatives

reported here therefore remains poorly understood, but indicates that for all exogenous labels this might be a more significant issue than previously considered.

The influence of exogenous labels on cell functions

The reliability of exogenous cells to identify transplanted cells has been the main focus of methodological studies (13), but potential effects on cellular functions have been mostly ignored, despite growing evidence to the contrary (68). The most dramatic effect observable is cell death due to acute or delayed toxicity. Although all labels here exhibited good viability (>90%) after cell labeling, indicating a lack of acute toxicity, Hoechst-labeled cells did not survive for 7 days revealing a delayed cytotoxicity. A thorough study by Pin et al. (51) showed that DNA binding agents did not exert their toxic effects on the nucleus, but instead had direct toxic effects on neurites via the RNA present within them. This is also supported by our observation that endothelial cells were unaffected by Hoechst labeling. PKH26 showed a minor reduction in viability straight after labeling, but this is likely due to the suspension labeling method retaining more dead cells compared to labeling attached cells. Although exposure to light of PKH26-labeled cells can induce phototoxicity (45), there was no evidence here that light modulated toxicity for any of the labels. For Qtracker-labeled cells, the exact molecular composition of these nanoparticles can influence toxicity (76), but there was no evidence of toxicity here. A previously reported selective neural toxicity of BrdU (9) was not evident here, possibly due to the use of lower concentrations of BrdU. Acute and delayed toxicity are hence essential reporters of cellular effects caused by exogenous labels that potentially invalidate their use to identify transplanted cells.

The incorporation of the exogenous label into different cellular compartments can further influence particular cellular functions, such as mitosis (i.e. cell proliferation). Cell division is a cardinal feature of NSCs. Hoechst and PKH26 both reduced proliferation acutely. Hoechst is known to cause DNA damage, as well as free radicals that lead to mutagenesis and free radical production, which all interfere with a normal cell cycle (14,15,53). Although cell proliferation in PKH26 cells normalized, a significant decrease initially could still reduce the overall amount of cells present after transplantation. In contrast, BrdU and Qtracker increased proliferation acutely before normalizing. Although BrdU has been reported to affect the cell cycle at higher concentrations (28), this was not evident here. These results indicate that all exogenous labels acutely affected proliferation, but there was no evidence of long-term effects.

A further key feature of NSCs is their ability to differentiate into neurons, astrocytes and oligodendrocytes. Neuronal differentiation was not affected by BrdU, PKH26 or Qtracker labeling. BrdU has been reported to affect both neuronal and oligodendrocytic, but not astrocytic, differentiation in adult rat NPCs (28). However, the BrdU protocol used here on fetal human NSCs resulted in a decrease of astrocytes and an increase in oligodendrocytes. It is possible that this difference is cell type dependent, or is a BrdU concentration-dependent effect, which has been shown to selectively affect neural progenitors (9). Qtracker also led to a major (20%) upregulation of GFAP with a minor (8%) decrease in GalC at 7 days. However, others have not reported any effect of quantum dots (34,62). In contrast, PKH26 did not significantly affect cell differentiation, other than astrocytic morphology. The mechanism by which PKH26 and Qtracker affect cell phenotype is unknown, but warrants further investigation in order to improve the design of future labels. It can be expected that BrdU induces conformational changes in the DNA structure (17) leading to more pronounced effects on cellular functions, compared to material localized within the cytoplasm or membrane. If these functions are deemed to be essential to therapeutic efficacy, more detailed studies are required prior to the use of these exogenous agents for cell transplantation studies.

Scope and limitations of cell labeling studies

Our results here indicate that exogenous labels result in a similarly reliable in vivo identification of implanted human NSCs in the absence of in vitro toxicity. These results potentially apply to NSCs more generally, including those derived from the spinal cord, although we previously noted subtle difference in using the same label on different brain-derived NSCs (4). Still, based on the results presented here, it remains unclear if these labels would achieve a comparable tolerance, efficiency and identification potential if other cells are used. Optimization and validation is highly recommended for each label and cell type (38). Importantly, we noted for instance that the Hoechst concentration used here was well tolerated by human endothelial cells (ECs), although it exerted a delayed toxicity in NSCs. We previously demonstrated that human ECs are more tolerant to exogenous labels compared to NSCs, potentially indicating a more general difference between these two cell types (43).

A further consideration is that the same cell type from different species could have different uptake or tolerance (25). Nevertheless, the labels used here have been used widely in NSCs of different species for cell transplantation studies (19,40,49). A direct comparison of NSCs from different species would hence be required to directly address

this issue. Intracellular tolerance of the label is not only dependent on its direct toxicity, but is also determined if it is degraded into potential toxic components that could have delayed effects (67). NSCs are known to be particularly fragile cells and provide a very sensitive system to probe toxicity (25,68), but this also poses a challenge, as intracerebral implantation requires NSCs' long-term survival. In contrast, identification or tracking of other cell types, such as mesenchymal cells or lymphocytes (2,22), is much shorter and hence labels, such as Hoechst, might still be suitable. A further evaluation of suitable labels for long-term identification of intracerebral transplantation hence requires an investigation of label retention, cell survival and phenotypic differentiation at longer time points in conjunction with behavioral analysis (37,68).

Conclusion

The interpretation of cell transplantation experiments is often dependent on the identification based on exogenous labels. We here demonstrated that Hoechst33342 is an inappropriate label for this purpose, whereas BrdU, PKH26 and Qtracker are reliable with <2% false positive identification, although there is a major concern regarding false negatives. A further concern is the cellular effects these exogenous labels exert with both BrdU and Qtracker exhibiting significant effects on proliferation and differentiation. The choice of an appropriate label therefore depends on the main purpose of the cell transplantation experiment. The studies reported here indicate that exogenous labels can be reliable to identify transplanted cells without exerting major cellular effects, but that validation is required and interpretations should be presented in the context of the label's limitations.

Acknowledgements

The authors acknowledge funding support by NINDS (R01NS082226) and the Commonwealth of Pennsylvania's Department of Health (4100061184). FN was supported by an MRC studentship.

Conflict of Interest Statement

The authors declare no conflict of interest related to this work.

References

1. Abordo-Adesida, E.; Follenzi, A.; Barcia, C.; Sciascia, S.; Castro, M. G.; Naldini, L.; Lowenstein, P. R. Stability of lentiviral vector-mediated transgene expression in the brain in the presence of systemic antivector immune responses. *Human gene therapy* 16(6):741-751; 2005.
2. Beem, E.; Segal, M. S. Evaluation of stability and sensitivity of cell fluorescent labels when used for cell migration. *J Fluoresc* 23(5):975-987; 2013.
3. Betz, W. J.; Mao, F.; Smith, C. B. Imaging exocytosis and endocytosis. *Current opinion in neurobiology* 6(3):365-371; 1996.
4. Bible, E.; Dell'Acqua, F.; Solanky, B.; Balducci, A.; Crapo, P. M.; Badylak, S. F.; Ahrens, E. T.; Modo, M. Non-invasive imaging of transplanted human neural stem cells and ECM scaffold remodeling in the stroke-damaged rat brain by (19)F- and diffusion-MRI. *Biomaterials* 33(10):2858-2871; 2012.
5. Brazelton, T. R.; Blau, H. M. Optimizing techniques for tracking transplanted stem cells in vivo. *Stem Cells* 23(9):1251-1265; 2005.
6. Brilli, E.; Reitano, E.; Conti, L.; Conforti, P.; Gulino, R.; Consalez, G. G.; Cesana, E.; Smith, A.; Rossi, F.; Cattaneo, E. Neural stem cells engrafted in the adult brain fuse with endogenous neurons. *Stem Cells Dev* 22(4):538-547; 2013.
7. Burns, T. C.; Ortiz-Gonzalez, X. R.; Gutierrez-Perez, M.; Keene, C. D.; Sharda, R.; Demorest, Z. L.; Jiang, Y.; Nelson-Holte, M.; Soriano, M.; Nakagawa, Y. and others. Thymidine analogs are transferred from prelabeled donor to host cells in the central nervous system after transplantation: a word of caution. *Stem Cells* 24(4):1121-1127; 2006.
8. Cadusseau, J.; Peschanski, M. Identifying grafted cells. *Neural transplantation: A practical approach*. Oxford, UK: Oxford University Press.; 1992:177-201.
9. Caldwell, M. A.; He, X.; Svendsen, C. N. 5-Bromo-2'-deoxyuridine is selectively toxic to neuronal precursors in vitro. *Eur J Neurosci* 22(11):2965-2970; 2005.
10. Chou, C. H.; Modo, M. Human neural stem cell-induced endothelial morphogenesis requires autocrine/paracrine and juxtacrine signaling. *Scientific reports* 6:29029; 2016.
11. Chou, C. H.; Sinden, J. D.; Couraud, P. O.; Modo, M. In vitro modeling of the neurovascular environment by coculturing adult human brain endothelial cells with human neural stem cells. *PLoS One* 9(9):e106346; 2014.
12. Crain, B. J.; Tran, S. D.; Mezey, E. Transplanted human bone marrow cells generate new brain cells. *Journal of the neurological sciences* 233(1-2):121-123; 2005.
13. Darkazalli, A.; Levenson, C. W. Tracking stem cell migration and survival in brain injury: current approaches and future prospects. *Histology and histopathology* 27(10):1255-1261; 2012.
14. Durand, R. E.; Olive, P. L. Cytotoxicity, Mutagenicity and DNA damage by Hoechst 33342. *The journal of histochemistry and cytochemistry : official journal of the Histochemistry Society* 30(2):111-116; 1982.
15. Erba, E.; Ubezio, P.; Broggin, M.; Ponti, M.; D'Incalci, M. DNA damage, cytotoxic effect and cell-cycle perturbation of Hoechst 33342 on L1210 cells in vitro. *Cytometry* 9(1):1-6; 1988.

16. Fang, C. Y.; Vaijayanthimala, V.; Cheng, C. A.; Yeh, S. H.; Chang, C. F.; Li, C. L.; Chang, H. C. The exocytosis of fluorescent nanodiamond and its use as a long-term cell tracker. *Small* 7(23):3363-3370; 2011.
17. Goz, B. The effects of incorporation of 5-halogenated deoxyuridines into the DNA of eukaryotic cells. *Pharmacological reviews* 29(4):249-272; 1977.
18. Gravier, J.; Navarro, F. P.; Delmas, T.; Mittler, F.; Couffin, A. C.; Vinet, F.; Texier, I. Lipidots: competitive organic alternative to quantum dots for in vivo fluorescence imaging. *Journal of biomedical optics* 16(9):096013; 2011.
19. Haas, S. J.; Bauer, P.; Rolfs, A.; Wree, A. Immunocytochemical characterization of in vitro PKH26-labelled and intracerebrally transplanted neonatal cells. *Acta histochemica* 102(3):273-280; 2000.
20. Harvey, A. R. Labeling and identifying grafted cells. In: Dunnett, S. B.; Baker, G. B., eds. *Neural Transplantation Methods*. Totowa, NJ: Humana Press; 2000:319-361.
21. Harvey, A. R.; Fan, Y.; Beilharz, M. W.; Grounds, M. D. Survival and migration of transplanted male glia in adult female mouse brains monitored by a Y-chromosome-specific probe. *Brain research. Molecular brain research* 12(4):339-343; 1992.
22. Hemmrich, K.; Meersch, M.; von Heimburg, D.; Pallua, N. Applicability of the dyes CFSE, CM-DiI and PKH26 for tracking of human preadipocytes to evaluate adipose tissue engineering. *Cells, tissues, organs* 184(3-4):117-127; 2006.
23. Iwashita, Y.; Crang, A. J.; Blakemore, W. F. Redistribution of bisbenzimidazole Hoechst 33342 from transplanted cells to host cells. *Neuroreport* 11(5):1013-1016; 2000.
24. Johansson, S.; Price, J.; Mado, M. Effect of inflammatory cytokines on major histocompatibility complex expression and differentiation of human neural stem/progenitor cells. *Stem Cells* 26(9):2444-2454; 2008.
25. Joris, F.; Valdeperez, D.; Pelaz, B.; Soenen, S. J.; Manshian, B. B.; Parak, W. J.; De Smedt, S. C.; Raemdonck, K. The impact of species and cell type on the nanosafety profile of iron oxide nanoparticles in neural cells. *J Nanobiotechnology* 14(1):69; 2016.
26. Krause, M.; Ganser, C.; Kobayashi, E.; Papazoglou, A.; Nikkhah, G. The Lewis GFP transgenic rat strain is a useful cell donor for neural transplantation. *Cell Transplant* 21(9):1837-1851; 2012.
27. Lassailly, F.; Griessinger, E.; Bonnet, D. "Microenvironmental contaminations" induced by fluorescent lipophilic dyes used for noninvasive in vitro and in vivo cell tracking. *Blood* 115(26):5347-5354; 2010.
28. Lehner, B.; Sandner, B.; Marschallinger, J.; Lehner, C.; Furtner, T.; Couillard-Despres, S.; Rivera, F. J.; Brockhoff, G.; Bauer, H. C.; Weidner, N. and others. The dark side of BrdU in neural stem cell biology: detrimental effects on cell cycle, differentiation and survival. *Cell and tissue research* 345(3):313-328; 2011.
29. Lepski, G.; Jannes, C. E.; Wessolleck, J.; Kobayashi, E.; Nikkhah, G. Equivalent neurogenic potential of wild-type and GFP-labeled fetal-derived neural progenitor cells before and after transplantation into the rodent hippocampus. *Transplantation* 91(4):390-397; 2011.

30. Li, K.; Qin, W.; Ding, D.; Tomczak, N.; Geng, J.; Liu, R.; Liu, J.; Zhang, X.; Liu, H.; Liu, B. and others. Photostable fluorescent organic dots with aggregation-induced emission (AIE dots) for noninvasive long-term cell tracing. *Scientific reports* 3:1150; 2013.
31. Li, N.; Yang, H.; Lu, L.; Duan, C.; Zhao, C.; Zhao, H. Comparison of the labeling efficiency of BrdU, Dil and FISH labeling techniques in bone marrow stromal cells. *Brain Res* 1215:11-19; 2008.
32. Li, P.; Zhang, R.; Sun, H.; Chen, L.; Liu, F.; Yao, C.; Du, M.; Jiang, X. PKH26 can transfer to host cells in vitro and vivo. *Stem Cells Dev* 22(2):340-344; 2013.
33. Libbus, B. L.; Perreault, S. D.; Johnson, L. A.; Pinkel, D. Incidence of chromosome aberrations in mammalian sperm stained with Hoechst 33342 and UV-laser irradiated during flow sorting. *Mutation research* 182(5):265-274; 1987.
34. Lin, S.; Xie, X.; Patel, M. R.; Yang, Y. H.; Li, Z.; Cao, F.; Gheysens, O.; Zhang, Y.; Gambhir, S. S.; Rao, J. H. and others. Quantum dot imaging for embryonic stem cells. *BMC biotechnology* 7:67; 2007.
35. Liu, S. J.; Zou, Y.; Belegu, V.; Lv, L. Y.; Lin, N.; Wang, T. Y.; McDonald, J. W.; Zhou, X.; Xia, Q. J.; Wang, T. H. Co-grafting of neural stem cells with olfactory ensheathing cells promotes neuronal restoration in traumatic brain injury with an anti-inflammatory mechanism. *Journal of neuroinflammation* 11:66; 2014.
36. Mao, X. G.; Hutt-Cabezas, M.; Orr, B. A.; Weingart, M.; Taylor, I.; Rajan, A. K.; Odia, Y.; Kahlert, U.; Maciaczyk, J.; Nikkhah, G. and others. LIN28A facilitates the transformation of human neural stem cells and promotes glioblastoma tumorigenesis through a pro-invasive genetic program. *Oncotarget* 4(7):1050-1064; 2013.
37. Modo, M.; Beech, J. S.; Meade, T. J.; Williams, S. C.; Price, J. A chronic 1 year assessment of MRI contrast agent-labelled neural stem cell transplants in stroke. *Neuroimage* 47 Suppl 2:T133-142; 2009.
38. Modo, M.; Kolosnjaj-Tabi, J.; Nicholls, F.; Ling, W.; Wilhelm, C.; Debarge, O.; Gazeau, F.; Clement, O. Considerations for the clinical use of contrast agents for cellular MRI in regenerative medicine. *Contrast Media Mol Imaging* 8(6):439-455; 2013.
39. Modo, M.; Rezaie, P.; Heuschling, P.; Patel, S.; Male, D. K.; Hodges, H. Transplantation of neural stem cells in a rat model of stroke: assessment of short-term graft survival and acute host immunological response. *Brain Res* 958(1):70-82; 2002.
40. Modo, M.; Stroemer, R. P.; Tang, E.; Patel, S.; Hodges, H. Effects of implantation site of stem cell grafts on behavioral recovery from stroke damage. *Stroke* 33(9):2270-2278; 2002.
41. Molcanyi, M.; Bosche, B.; Kraitsy, K.; Patz, S.; Zivcak, J.; Riess, P.; El Majdoub, F.; Hescheler, J.; Goldbrunner, R.; Schafer, U. Pitfalls and fallacies interfering with correct identification of embryonic stem cells implanted into the brain after experimental traumatic injury. *J Neurosci Methods* 215(1):60-70; 2013.
42. Moloney, T. C.; Dockery, P.; Windebank, A. J.; Barry, F. P.; Howard, L.; Dowd, E. Survival and immunogenicity of mesenchymal stem cells from the green fluorescent protein transgenic rat in the adult rat brain. *Neurorehabil Neural Repair* 24(7):645-656; 2010.

43. Nicholls, F. J.; Ling, W.; Ferrauto, G.; Aime, S.; Modo, M. Simultaneous MR imaging for tissue engineering in a rat model of stroke. *Scientific reports* 5:14597; 2015.
44. Nicholls, F. J.; Rotz, M. W.; Ghuman, H.; MacRenaris, K. W.; Meade, T. J.; Modo, M. DNA-gadolinium-gold nanoparticles for in vivo T1 MR imaging of transplanted human neural stem cells. *Biomaterials* 77:291-306; 2016.
45. Oh, D. J.; Lee, G. M.; Francis, K.; Palsson, B. O. Phototoxicity of the fluorescent membrane dyes PKH2 and PKH26 on the human hematopoietic KG1a progenitor cell line. *Cytometry* 36(4):312-318; 1999.
46. Parish, C. R. Fluorescent dyes for lymphocyte migration and proliferation studies. *Immunol Cell Biol* 77(6):499-508; 1999.
47. Pawelczyk, E.; Jordan, E. K.; Balakumaran, A.; Chaudhry, A.; Gormley, N.; Smith, M.; Lewis, B. K.; Childs, R.; Robey, P. G.; Frank, J. A. In vivo transfer of intracellular labels from locally implanted bone marrow stromal cells to resident tissue macrophages. *PLoS One* 4(8):e6712; 2009.
48. Pereira Lopes, F. R.; Frattini, F.; Marques, S. A.; Almeida, F. M.; de Moura Campos, L. C.; Langone, F.; Lora, S.; Borojevic, R.; Martinez, A. M. Transplantation of bone-marrow-derived cells into a nerve guide resulted in transdifferentiation into Schwann cells and effective regeneration of transected mouse sciatic nerve. *Micron* 41(7):783-790; 2010.
49. Pettersson, J.; Lobov, S.; Novikova, L. N. Labeling of olfactory ensheathing glial cells with fluorescent tracers for neurotransplantation. *Brain Res Bull* 81(1):125-132; 2010.
50. Pierzynska-Mach, A.; Janowski, P. A.; Dobrucki, J. W. Evaluation of acridine orange, LysoTracker Red, and quinacrine as fluorescent probes for long-term tracking of acidic vesicles. *Cytometry. Part A : the journal of the International Society for Analytical Cytology* 85(8):729-737; 2014.
51. Pin, S.; Chen, H.; Lein, P. J.; Wang, M. M. Nucleic acid binding agents exert local toxic effects on neurites via a non-nuclear mechanism. *J Neurochem* 96(5):1253-1266; 2006.
52. Pollock, K.; Stroemer, P.; Patel, S.; Stevanato, L.; Hope, A.; Miljan, E.; Dong, Z.; Hodges, H.; Price, J.; Sinden, J. D. A conditionally immortal clonal stem cell line from human cortical neuroepithelium for the treatment of ischemic stroke. *Experimental neurology* 199(1):143-155; 2006.
53. Poot, M.; Rudiger, H. W.; Hoehn, H. Detection of free radical-induced DNA damage with bromodeoxyuridine/Hoechst flow cytometry: implications for Bloom's syndrome. *Mutation research* 238(3):203-207; 1990.
54. Progatzy, F.; Dallman, M. J.; Lo Celso, C. From seeing to believing: labelling strategies for in vivo cell-tracking experiments. *Interface focus* 3(3):20130001; 2013.
55. Ranganathan, S.; Churchill, P. F.; Hood, R. D. Inhibition of mitochondrial respiration by cationic rhodamines as a possible teratogenicity mechanism. *Toxicology and applied pharmacology* 99(1):81-89; 1989.
56. Rossetti, T.; Nicholls, F.; Modo, M. Intracerebral Cell Implantation: Preparation and Characterization of Cell Suspensions. *Cell Transplant* 25(4):645-664; 2016.

57. Rossignol, J.; Boyer, C.; Leveque, X.; Fink, K. D.; Thinard, R.; Blanchard, F.; Dunbar, G. L.; Lescaudron, L. Mesenchymal stem cell transplantation and DMEM administration in a 3NP rat model of Huntington's disease: morphological and behavioral outcomes. *Behav Brain Res* 217(2):369-378; 2011.
58. Rossignol, J.; Boyer, C.; Thinard, R.; Remy, S.; Dugast, A. S.; Dubayle, D.; Dey, N. D.; Boeffard, F.; Delecryn, J.; Heymann, D. and others. Mesenchymal stem cells induce a weak immune response in the rat striatum after allo or xenotransplantation. *Journal of cellular and molecular medicine* 13(8B):2547-2558; 2009.
59. Saetzler, R. K.; Jallo, J.; Lehr, H. A.; Philips, C. M.; Vasthare, U.; Arfors, K. E.; Tuma, R. F. Intravital fluorescence microscopy: impact of light-induced phototoxicity on adhesion of fluorescently labeled leukocytes. *The journal of histochemistry and cytochemistry : official journal of the Histochemistry Society* 45(4):505-513; 1997.
60. Samlowski, W. E.; Robertson, B. A.; Draper, B. K.; Prystas, E.; McGregor, J. R. Effects of supravital fluorochromes used to analyze the in vivo homing of murine lymphocytes on cellular function. *Journal of immunological methods* 144(1):101-115; 1991.
61. Sanchez-Ramos, J.; Song, S.; Dailey, M.; Cardozo-Pelaez, F.; Hazzi, C.; Stedeford, T.; Willing, A.; Freeman, T. B.; Saporta, S.; Zigova, T. and others. The X-gal caution in neural transplantation studies. *Cell Transplant* 9(5):657-667; 2000.
62. Shang, W.; Zhang, X.; Zhang, M.; Fan, Z.; Sun, Y.; Han, M.; Fan, L. The uptake mechanism and biocompatibility of graphene quantum dots with human neural stem cells. *Nanoscale* 6(11):5799-5806; 2014.
63. Shiohara, A.; Hoshino, A.; Hanaki, K.; Suzuki, K.; Yamamoto, K. On the cytotoxicity caused by quantum dots. *Microbiology and immunology* 48(9):669-675; 2004.
64. Sinden, J. D.; Rashid-Doubell, F.; Kershaw, T. R.; Nelson, A.; Chadwick, A.; Jat, P. S.; Noble, M. D.; Hodges, H.; Gray, J. A. Recovery of spatial learning by grafts of a conditionally immortalized hippocampal neuroepithelial cell line into the ischaemia-lesioned hippocampus. *Neuroscience* 81(3):599-608; 1997.
65. Smith, E. J.; Stroemer, R. P.; Gorenkova, N.; Nakajima, M.; Crum, W. R.; Tang, E.; Stevanato, L.; Sinden, J. D.; Modo, M. Implantation site and lesion topology determine efficacy of a human neural stem cell line in a rat model of chronic stroke. *Stem Cells* 30(4):785-796; 2012.
66. Snyder, E. Y.; Deitcher, D. L.; Walsh, C.; Arnold-Aldea, S.; Hartwig, E. A.; Cepko, C. L. Multipotent neural cell lines can engraft and participate in development of mouse cerebellum. *Cell* 68(1):33-51; 1992.
67. Soenen, S. J.; Abe, S.; Manshian, B. B.; Aubert, T.; Hens, Z.; De Smedt, S. C.; Braeckmans, K. The Effect of Intracellular Degradation on Cytotoxicity and Cell Labeling Efficacy of Inorganic Ligand-Stabilized Colloidal CdSe/CdS Quantum Dots. *J Biomed Nanotechnol* 11(4):631-643; 2015.
68. Soenen, S. J.; Rivera-Gil, P.; Montenegro, J. M.; Parak, W. J.; De Smedt, S. C.; Braeckmans, K. Cellular toxicity of inorganic nanoparticles: Common aspects

- and guidelines for improved nanotoxicity evaluation. *Nano Today* 6(5):446-465; 2011.
69. Spitzer, N.; Sammons, G. S.; Price, E. M. Autofluorescent cells in rat brain can be convincing impostors in green fluorescent reporter studies. *J Neurosci Methods* 197(1):48-55; 2011.
 70. Sprick, U. Long-term tracing of vital neurons with Hoechst 33342 in transplantation studies. *J Neurosci Methods* 36(2-3):229-238; 1991.
 71. Taupin, P. BrdU immunohistochemistry for studying adult neurogenesis: paradigms, pitfalls, limitations, and validation. *Brain Res Rev* 53(1):198-214; 2007.
 72. Tornero, D.; Wattananit, S.; Gronning Madsen, M.; Koch, P.; Wood, J.; Tatarishvili, J.; Mine, Y.; Ge, R.; Monni, E.; Devaraju, K. and others. Human induced pluripotent stem cell-derived cortical neurons integrate in stroke-injured cortex and improve functional recovery. *Brain* 136(Pt 12):3561-3577; 2013.
 73. Trumble, T. E.; Parvin, D. Cell viability and migration in nerve isografts and allografts. *Journal of reconstructive microsurgery* 10(1):27-34; 1994.
 74. Vega, M. C.; Garcia Saez, I.; Aymami, J.; Eritja, R.; Van der Marel, G. A.; Van Boom, J. H.; Rich, A.; Coll, M. Three-dimensional crystal structure of the A-tract DNA dodecamer d(CGCAAATTTGCG) complexed with the minor-groove-binding drug Hoechst 33258. *Eur J Biochem* 222(3):721-726; 1994.
 75. Weksler, B. B.; Subileau, E. A.; Perriere, N.; Charneau, P.; Holloway, K.; Leveque, M.; Tricoire-Leignel, H.; Nicotra, A.; Bourdoulous, S.; Turowski, P. and others. Blood-brain barrier-specific properties of a human adult brain endothelial cell line. *FASEB journal : official publication of the Federation of American Societies for Experimental Biology* 19(13):1872-1874; 2005.
 76. Yong, K. T.; Law, W. C.; Hu, R.; Ye, L.; Liu, L.; Swihart, M. T.; Prasad, P. N. Nanotoxicity assessment of quantum dots: from cellular to primate studies. *Chemical Society reviews* 42(3):1236-1250; 2013.
 77. Zhang, S.; Zou, Z.; Jiang, X.; Xu, R.; Zhang, W.; Zhou, Y.; Ke, Y. The therapeutic effects of tyrosine hydroxylase gene transfected hematopoietic stem cells in a rat model of Parkinson's disease. *Cellular and molecular neurobiology* 28(4):529-543; 2008.
 78. Zhao, W.; Dong, S.; Sun, L.; Wang, Q.; Gai, H. Investigating the Photostability of Quantum Dots at the Single-Molecule Level. *Chemistry, an Asian journal*; 2014.

Figures

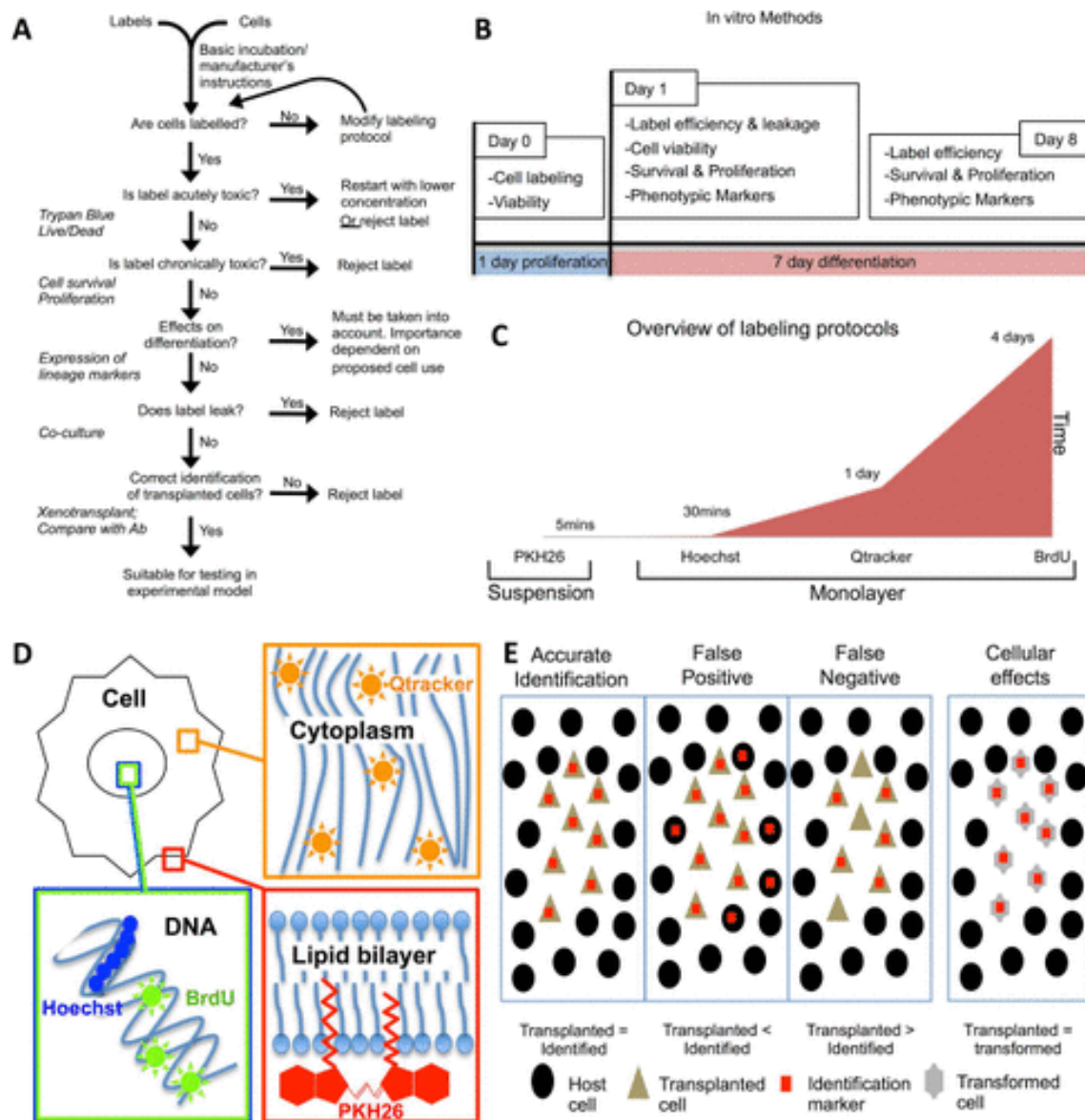


Figure 1. Experimental Design. (A) Investigative flow-chart to determine if labels affect cellular function and provide a reliable identification of transplanted cells. (B) Overview of in vitro experiments to determine cellular effects of labeling. On Day 0, cells are labeled using the various methods and acute toxicity is determined using viability measures. On Day 1, the efficiency of labeling (% cells labeled), viability (% alive/dead at that moment), survival (cell numbers) and phenotypic characteristics are determined. To ensure persistence of the label without ill effects, the number of cells remaining labeled (efficiency), survival and proliferation, as well as potential impact on phenotypic differentiation are evaluated on day 8. (C) Overview of labeling methods in terms of culture

conditions and time used for labeling. PKH26 in contrast to the other methods is a short labeling protocol performed in suspension. Hoechst requires a relatively short labeling period while cells are growing, whereas BrdU which only gets incorporated into cells in S phase requires 4 days of labeling to ensure that a sufficiently high percentage of cells are actually labeled. These methodological differences further affect the potential use of a particular approach. **(D)** Exogenous labels integrate into different intracellular locations. PK26 integrates into the cell membrane, Qtracker into the cytoplasm, whereas Hoechst and BrdU insert into DNA in the nucleus. **(E)** Principles of identifying correctly labeled cells versus false positives (labeled host cells, Type I error, specificity) and negatives (unlabeled implanted cells, Type II error, sensitivity), as well as potential effects of cell labeling on cell labeling (e.g. differentiation).

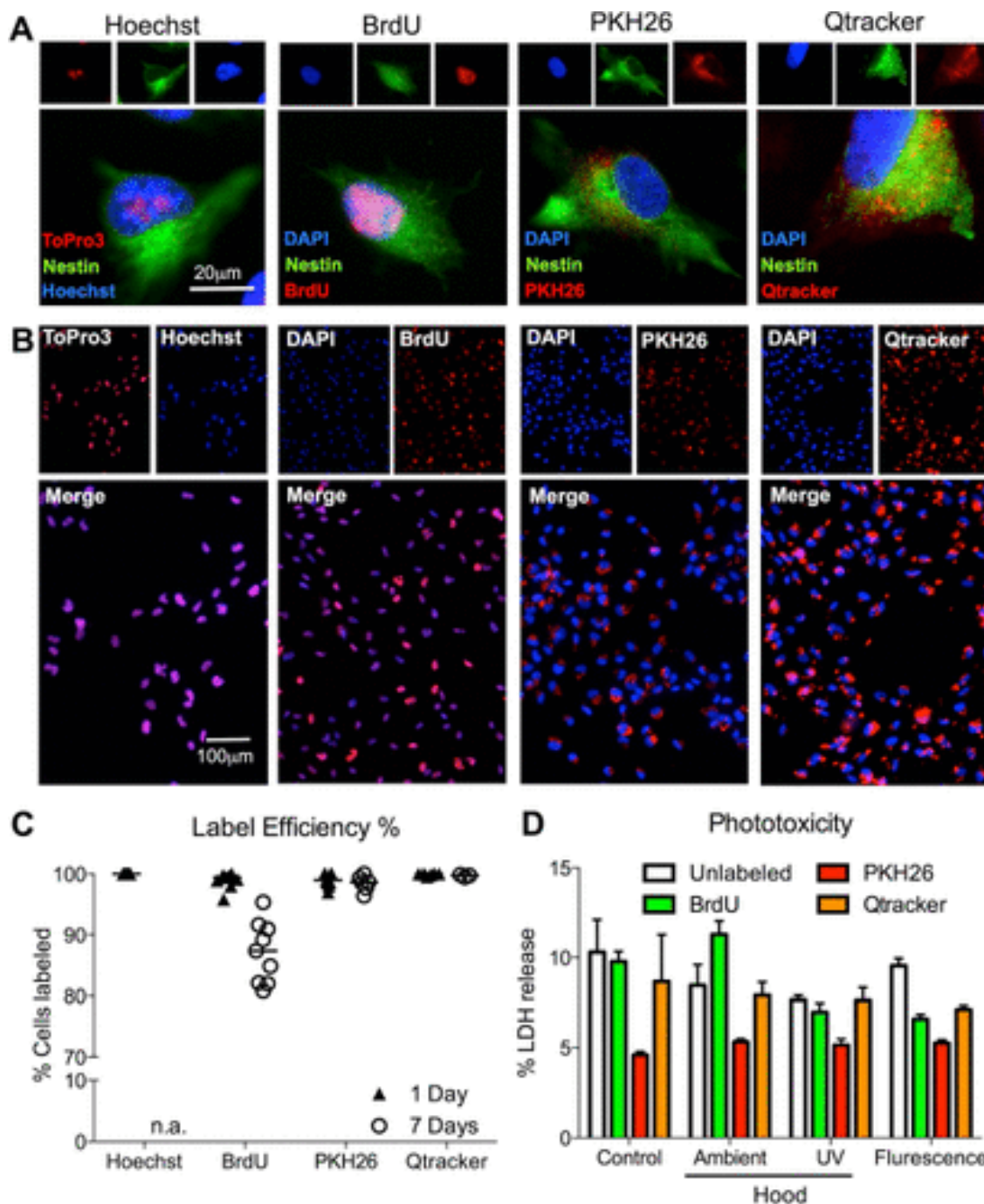


Figure 2. Efficiency of cell labeling. **(A)** Visualization of exogenous labels in a single cell. It is evident that Hoechst and BrdU show an intra-nuclear localization, whereas PKH26 and Qtracker are distributed throughout the cytoplasm of the cell. **(B)** A population view of labeled cells further indicates differences in the appearance of the labels with nuclear markers being easier to ascribe to a cell than cytoplasmic markers. **(C)** The percentage of labeled cells at day 1 and day 7 indicates that immediately after labeling Hoechst, BrdU, PKH26 and Qtracker achieved an almost complete labeling. However, by

7 days, no Hoechst labeled cells were present anymore (due to cell death) and the number of BrdU-labeled cells further reduced to a median of 87% ($p < .001$). PKH26 and Qtracker still afforded detection of almost all cells.

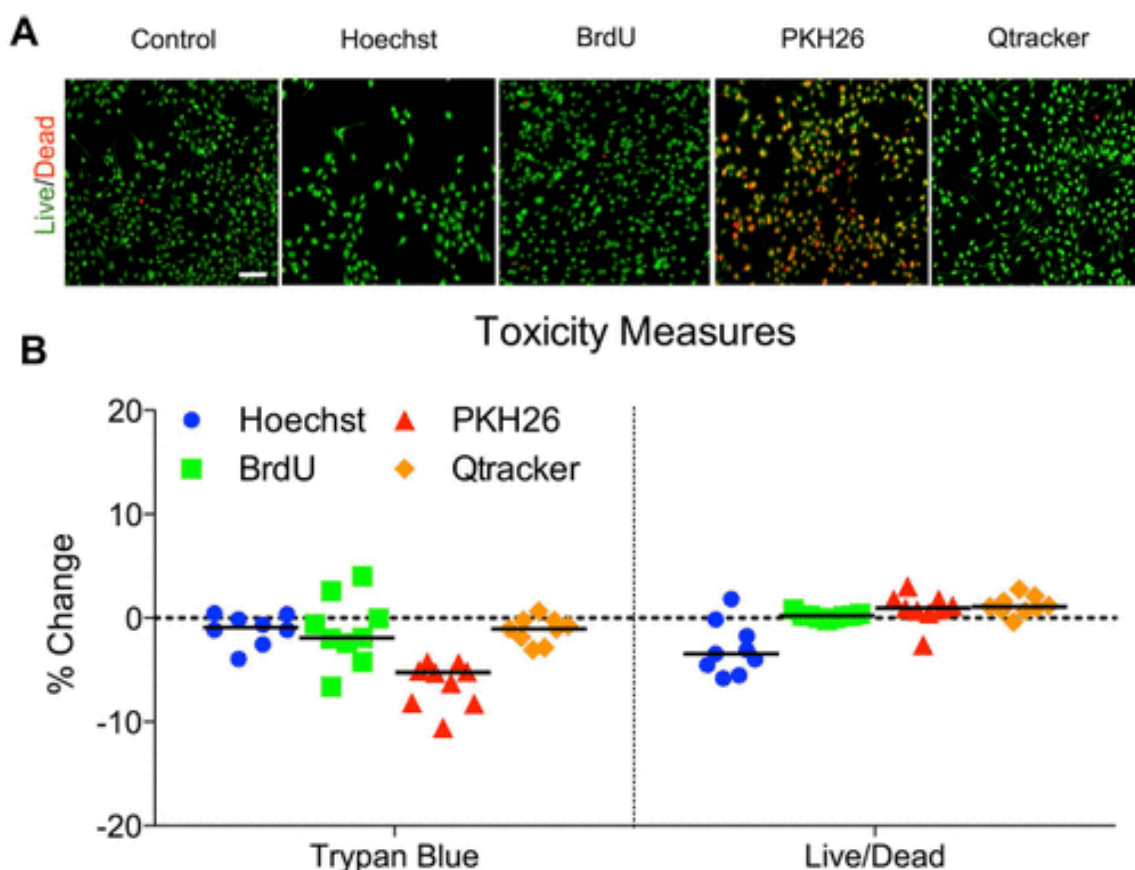


Figure 3. Toxicity due to cell labeling. (A) Assessment of cell viability using Live/Dead staining afforded a quantification of both fractions of cells. For PKH26 and Qtracker, the cell label occupied the same channel as EthD-1, the marker of dead cells. However, EthD-1 is nuclear, and could therefore be distinguished from the labels based on localization. Additionally, live cells could still easily be distinguished by green Calcein-AM. **(B)** Quantification of viability after cell labeling with trypan blue measured potential toxicity effects during labeling. There was no effect of cellular toxicity due to Hoechst, BrdU or Qtracker in comparison to unlabeled cells undergoing the same procedure. PKH26 was slightly (6.4%) reduced ($p < .001$). At day 1, only Hoechst exhibited a slight (2.4%), yet non-significant, reduction in live cells. Scale bar = 100 μ m.

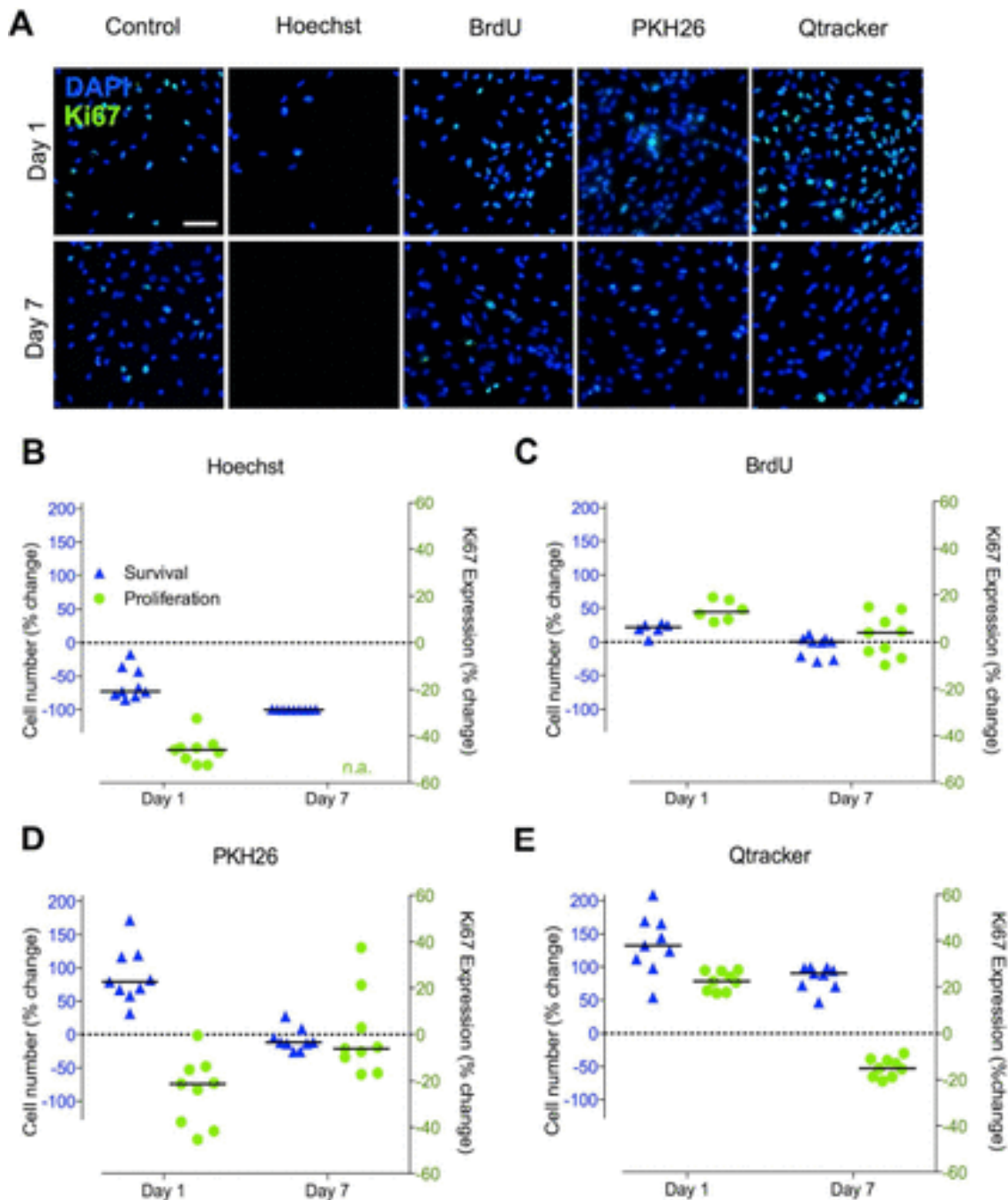


Figure 4. Cell survival and proliferation after cell labeling. (A) In contrast to viability, which measures what percentage of cells are alive/dead, survival measures how many cells in total are present at day 1 and day 7, hence potentially discerning low, but persistent, levels of cell death that might not be evident on measures of cell viability. To this end, all DAPI+ cells are counted, whereas to determine how many cells are proliferating the number of Ki67+ cells is considered. (B) The number of cells remaining after 24 hours with Hoechst was reduced by 75% and proliferation was down by 42%. By

7 days almost all cells had died. **(C)** BrdU led to an increase in proliferation at 1 day that was reflected in more cells being present than in control conditions. However, by 7 days this effect had normalized. **(D)** A decrease in proliferation was evident for PKH26, although more cells were present within the conditions compared to control, potentially indicating an early effect on proliferation that was reversed within 24 hours. By 7 days, again the effects normalized compared to controls. **(E)** Both proliferation and survival were increased for Qtracker after 24 hours, with survival remaining elevated compared to control at 7 days, although there was a slight decrease in proliferating cells. Scale bar = 100 μm .

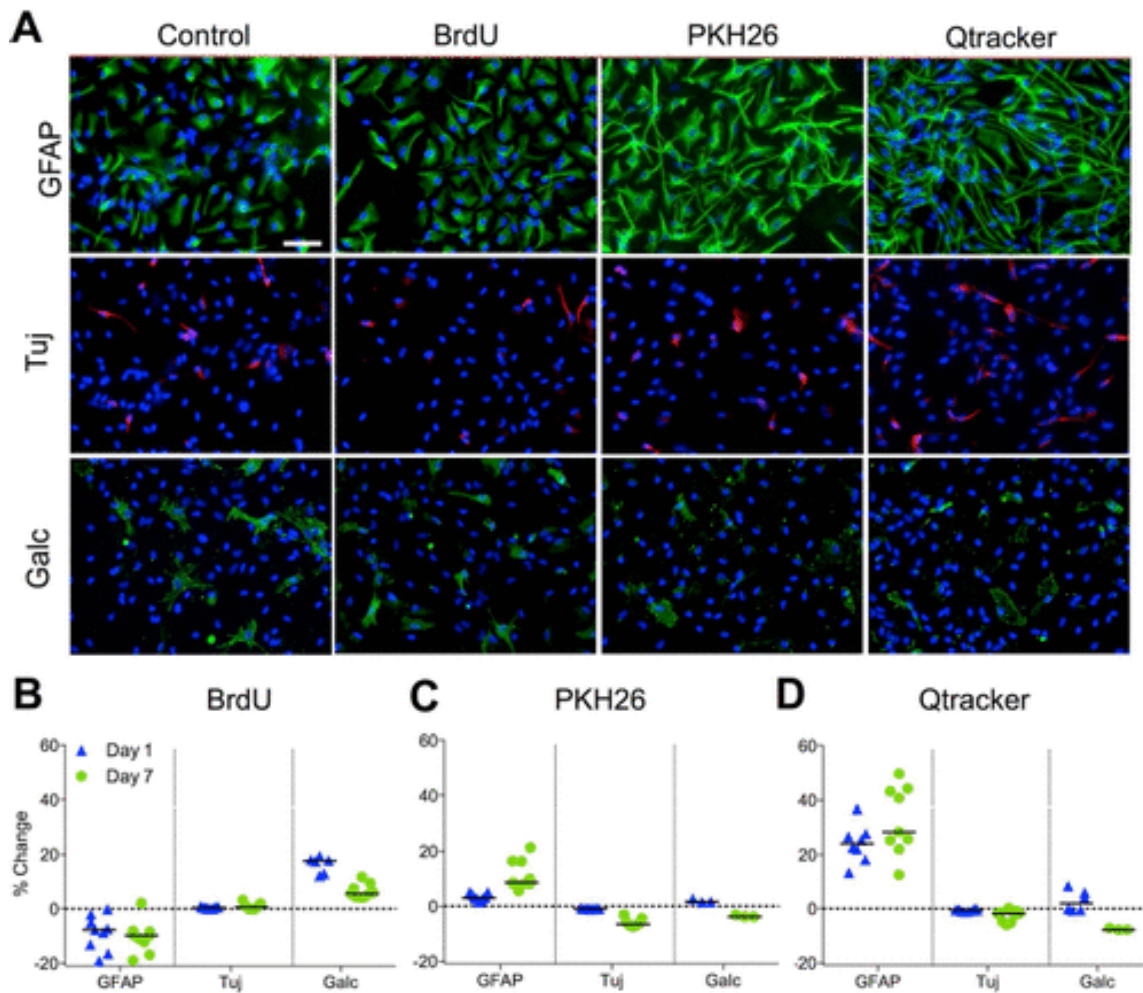


Figure 5. Cell differentiation after cell labeling. (A) 7 days of differentiation into the 3 cell lineages derived from NSCs: neurons (Tuj), astrocytes (GFAP) and oligodendrocytes (GalC). Note that Tuj and GalC are typically at very low levels in day 1 cultures, so decreases are unlikely. **(B)** BrdU had no effect on neuronal differentiation, but reduced astrocytic cell fate, while shifting differentiation towards an oligodendrocyte fate. **(C)** PKH26 slightly, yet non-significantly decreased neuronal and oligodendrocyte cell fate, while enhancing astrocytic cell fate. **(D)** Qtracker did not affect neuronal fate, but significantly increased astrocytic fate, while reducing oligodendrocyte fate. Scale bar = 100 μ m.

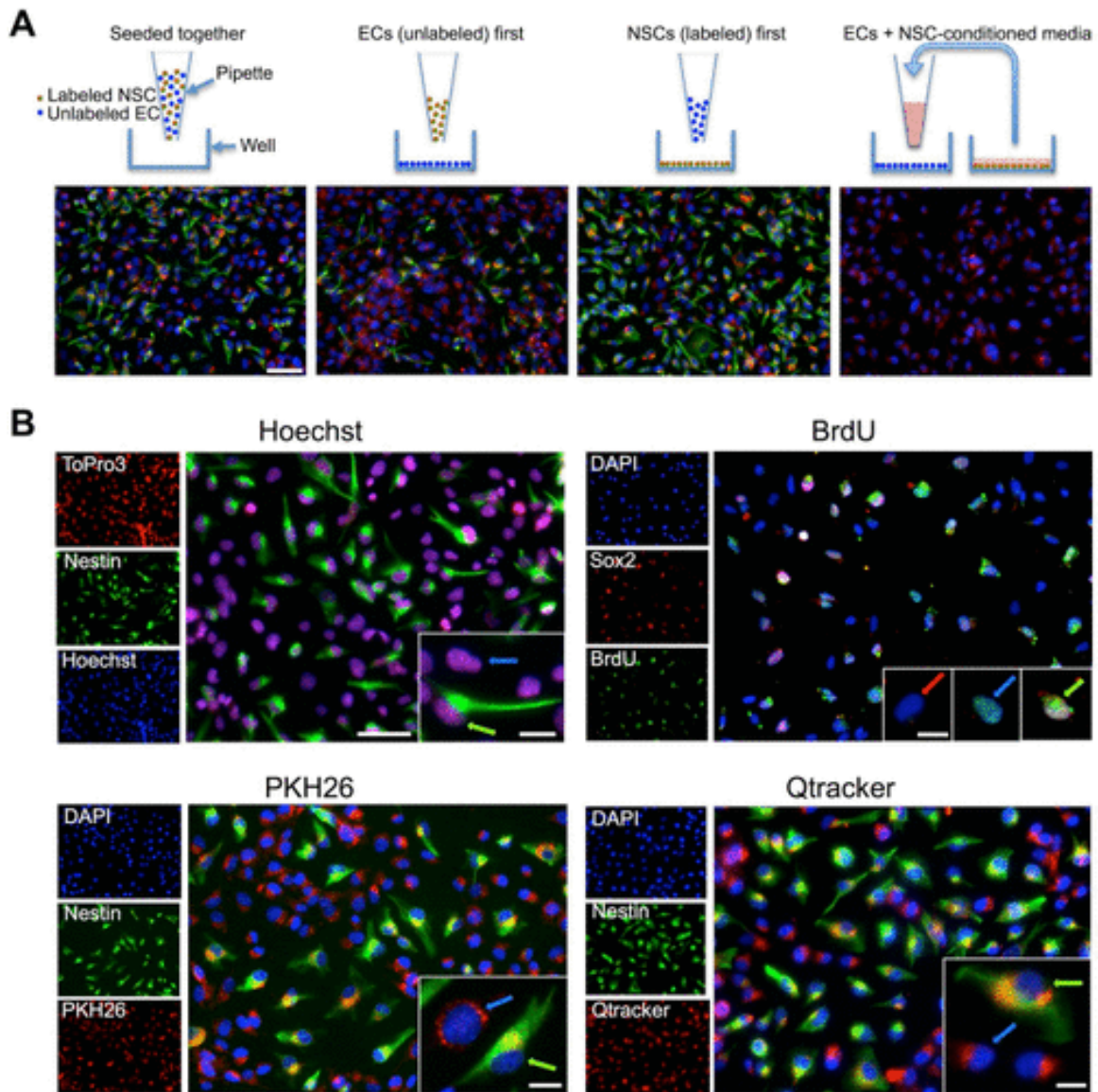


Figure 6. Leakage and re-uptake in vitro. (A) A co-culture of endothelial cells (ECs) and labeled hNSCs affords an investigation of the transfer of label from labeled to unlabeled cells. However, in vitro different set-ups for co-culture can potentially lead to transfer of label. PKH26-labeled hNSCs stained with nestin for identification of NSCs. DAPI served as counterstain for all cells. Regardless of the co-culture method, PKH26 was found in both hNSCs and ECs with a transfer rate of 100%. Only PKH26 is shown here as a representative label, but each label's results were consistent across setup conditions. Scale bar = 100 μ m, insets 25 μ m **(B)** Seeding of labeled hNSCs onto unlabeled ECs indicated that within 24 hours of co-culture there was significant transfer of label from hNSCs (green arrows) to ECs (blue arrows). Close to 100% of ECs contained Hoechst, PKH26, Qtracker, or BrdU, although a few ECs remained unlabeled with BrdU (red arrow).

hNSCs remained identifiable based on the exogenous label. Nestin or Sox2 (green) was used to label hNSCs. The procedure for BrdU interfered with Nestin staining and hence Sox2 was used instead to identify hNSCs.

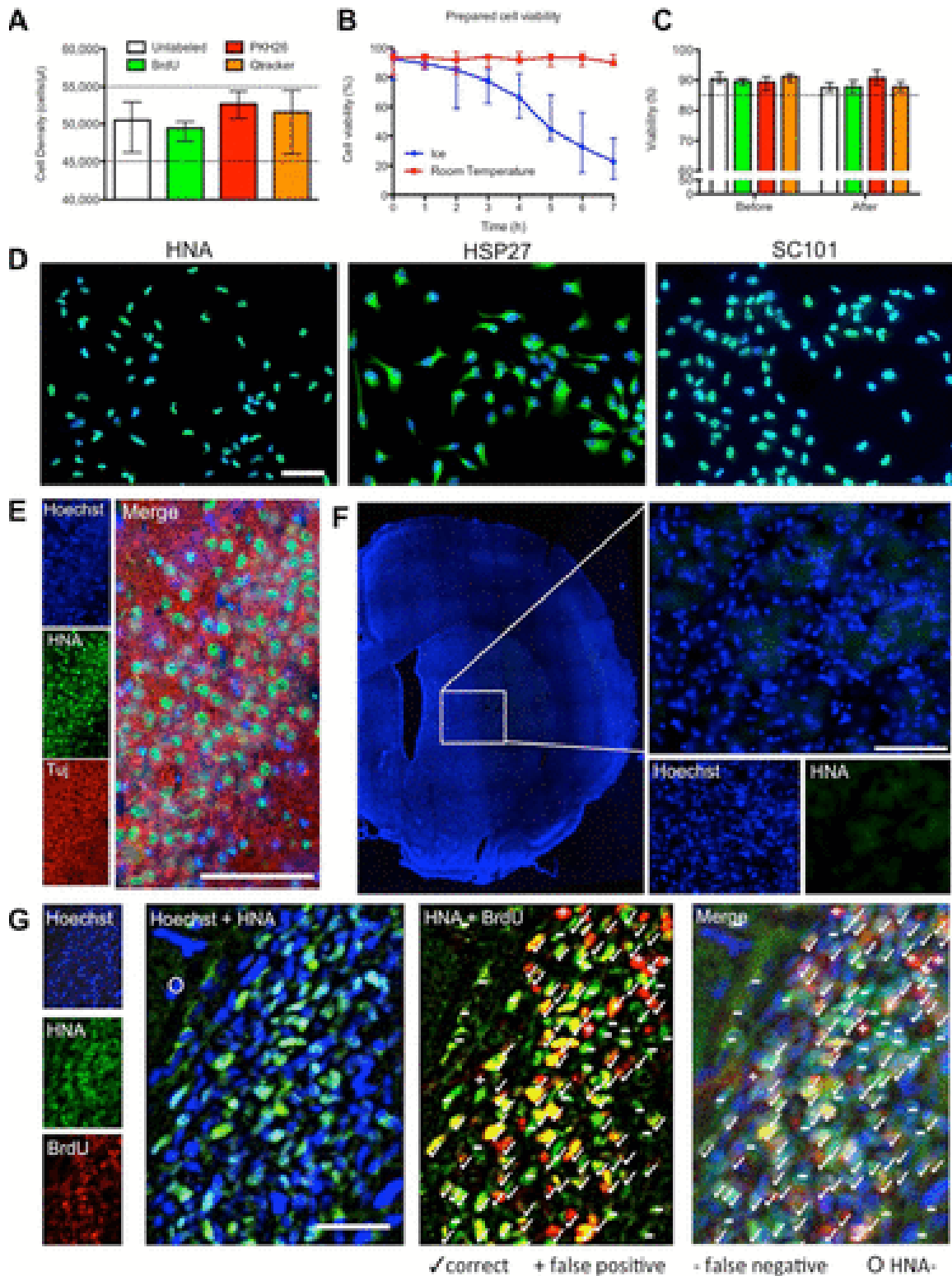


Figure 7. Quality Control. (A) Cell suspensions prepared for in vivo transplantation experiments fell within a 10% error margin (dotted lines) for all preparations, ensuring a consistent cell delivery. (B) To ensure a persistent viability, it was determined that

maintaining cells at room temperature was favorable compared to keeping cells on ice. **(C)** Cell suspensions were assessed for cell viability using Trypan Blue, before and after 4 hours of transplant surgery. Viability remained above 85% (dotted line) for all preparations used for in vivo experiments. **(D)** Three human specific antibodies (all green), human nuclei antigen (HNA), human-specific heat shock protein 27 (HSP27), and a human nuclei specific antibody (SC101) were tested for their ability to label all hNSCs in vitro, and all achieved 100% (DAPI=blue). **(E)** Each individual cell nucleus in a human tissue sample (i.e. positive control) from an adult hippocampus stains positive for HNA (HNA=green; Tuj=red; Hoechst=blue; Scale bar represents 100 μ m). **(F)** The normal rat brain (i.e. negative control) does not show any reactivity with these human-specific antibodies, as indicated here for HNA. (HNA=green; Hoechst-blue; Scale bar represents 200 μ m). **(G)** Image analysis, shown here with BrdU labeled cells, and symbols showing which cells would be counted as correctly identified (tick, labeled transplanted cell), false positive (+, labeled host cells) and false negative (-, unlabeled transplanted cells). An example is also shown of a cell with some green background that would be classified as HNA- (O).

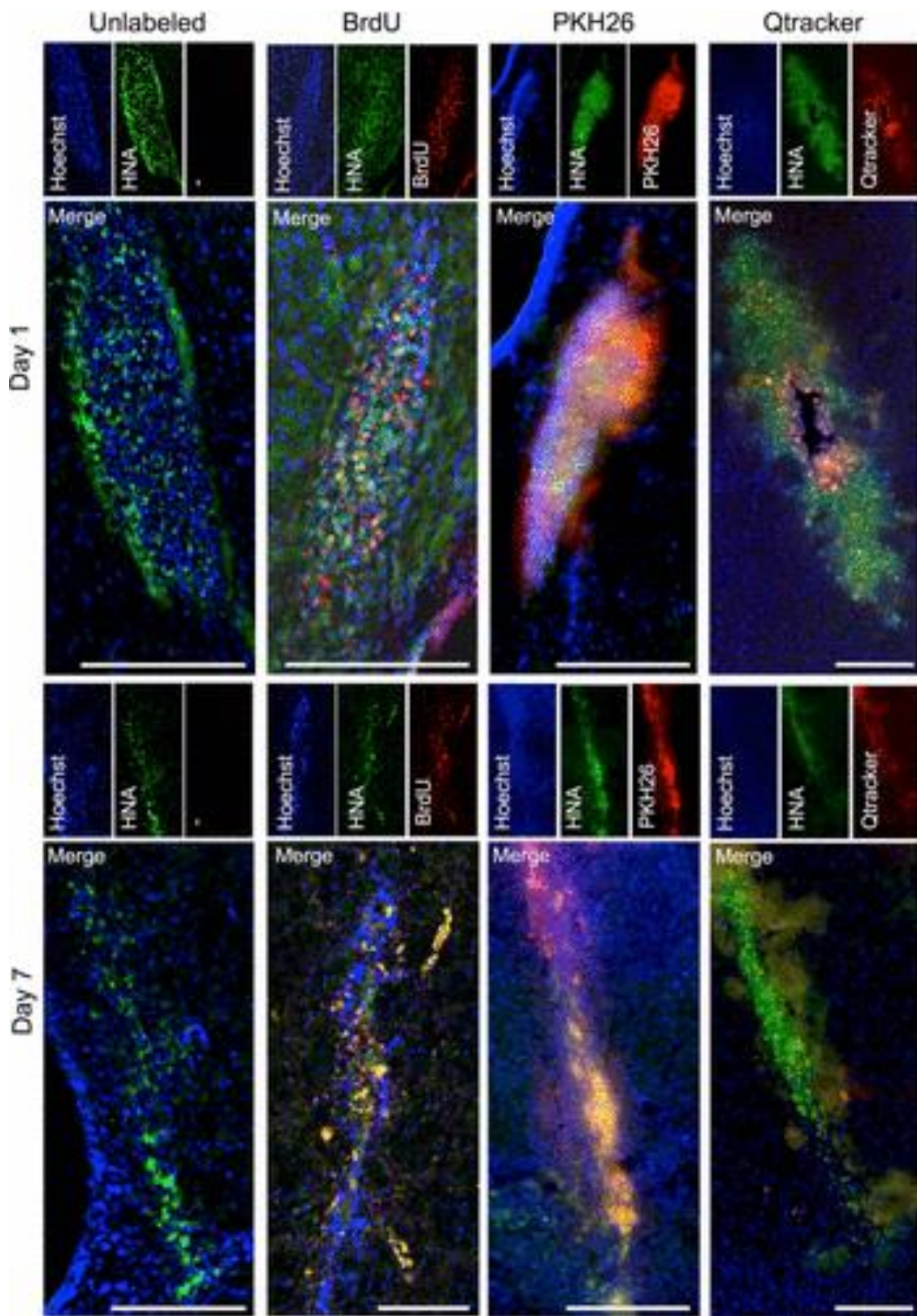


Figure 8. Histological characteristics of cellular grafts. Considerable differences in graft appearance based on cell labeling were evident. At Day 1, HNA+ transplanted cells

survived in all conditions and were confined to the deposit site. HNA afforded easy identification of cells in the unlabeled condition, and there was little evidence of autofluorescence in the red channel. BrdU in contrast was confined to the deposit site, but the immunohistochemical procedure used to detect BrdU lead to some HNA staining artifacts in the vicinity of the transplant site. PKH26 reliably defined the graft deposit, but the strong fluorescence in the red channel leached into the green channel and interfered with the detection of individual cells labeled with HNA. Qtracker did not induce a leach into the green channel, but the very punctate appearance of the qdots complicates identification of individual cells in the absence of a cytoplasmic marker. After 7 days of survival, BrdU was well localized to areas with HNA staining with no significant dispersion of the label evident beyond the distribution of HNA-stained cells. PKH26 was also confined to areas of HNA staining, although it remained difficult to identify individual cells in these areas based on PKH26 staining. However, there was less bleed through into the green channel than at day 1. There was no distribution of PKH26 beyond the transplant site. A similar pattern to PKH26 was observed for Qtracker, although there was no significant bleed through into the green channel.

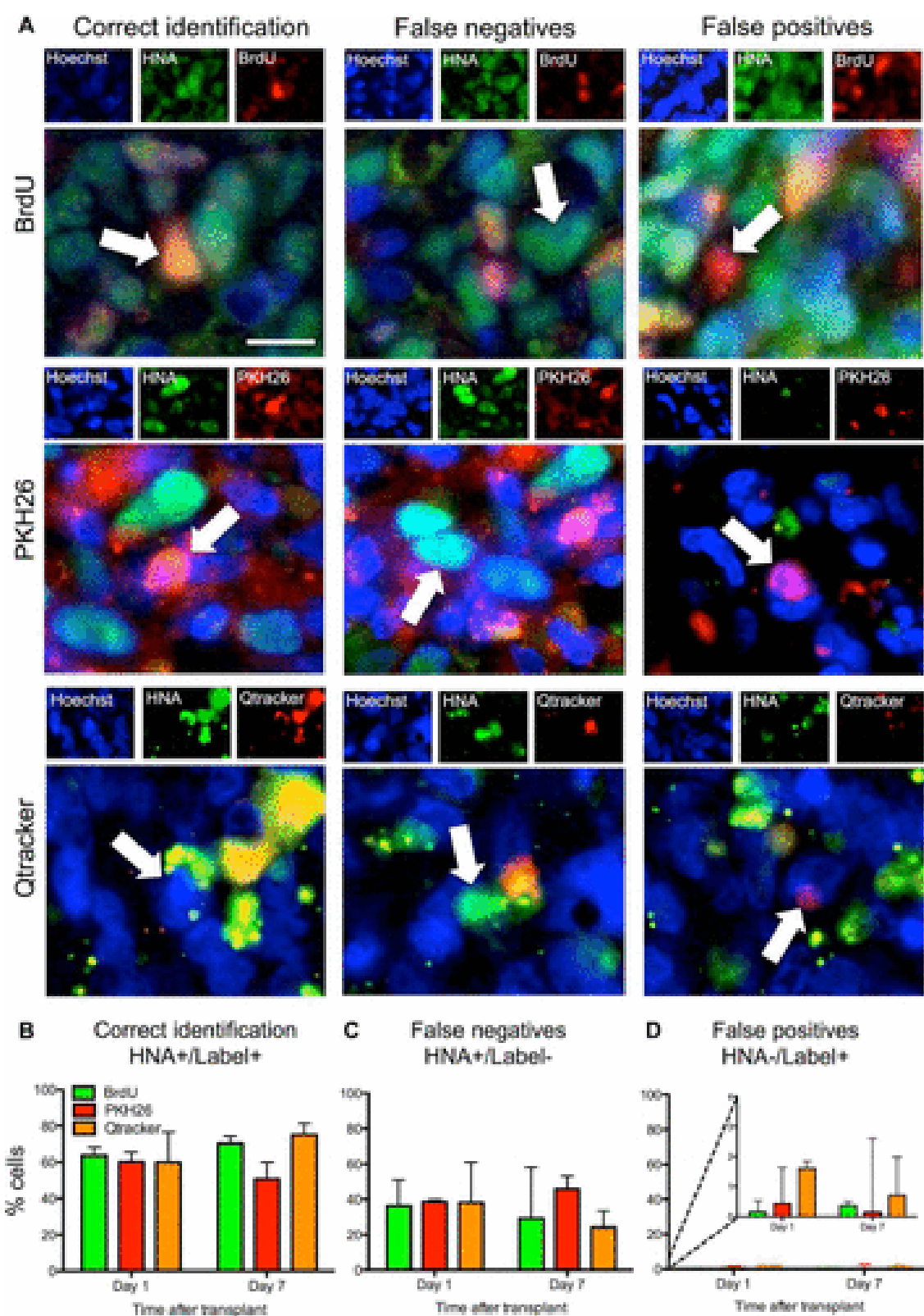


Figure 9. Accuracy of cell identification based on exogenous labels. (A) Quantification of reliable (correct) identification of cells based on their exogenous label, in

comparison to transplanted cells no longer identifiable based on the exogenous label (false negatives), and host cells containing an exogenous label (false positives). Sample images for each condition and label are presented. **(B)** On day 1, BrdU, PKH26 and Qtracker achieved approximately a 60% accurate identification of transplanted cells, whereas 7 days, this increased to ~70% for BrdU and Qtracker and reduced to 50% for PKH26. **(C)** A significant portion (>30%) of implanted cells were no longer identifiable based on their exogenous marker at both 1 and 7 days post-implantation. However, this proportion was fairly stable, although it was significantly increased for PKH26 and potentially explains the decrease in correct identification of PKH26 labeled cells at day 7. **(D)** The proportion of cells that were misidentified as transplanted cells was surprisingly insignificant (<2%) for BrdU, PKH26 and Qtracker.